Waterproof Flexible InP@ZnSeS Quantum dot Light-Emitting Diode

Dong-Wook Shin‡, Yo-Han Suh‡, Sanghyo Lee, Bo Hou, Soo Deok Han, Yuljae Cho, Xiangbing Fan, Sang Yun Bang, Shijie Zhan, Jiajie Yang, Hyung Woo Choi, Sungmin Jung, Felix Mocanu, Hanleem Lee, Luigi Occhipinti, Young Tea Chun, Gehan Amaratunga, Jong Min Kim*

Dr D-W. Shin, Dr Y-H. Suh, Dr S. Lee, Dr B. Hou, Dr S. Han, Dr Y. Cho, Dr X. Fan, S. Y. Bang, S. Zhan, J. Yang, Dr H. W. Choi, Dr S. Jung, F. Mocanu, Dr H. Lee, Dr L. Occhipiniti, Dr Y. T. Chun, Prof. G. Amaratunga, Prof. J. M. Kim
Electrical Engineering Division, Department of Engineering, University of Cambridge, 9 JJ Thomson Avenue, Cambridge, CB3 0FA, UK
‡Those authors contributed equally to this work
E-mail: ytc24@cam.ac.uk

Keywords: InP@ZnSeS; photoluminescence quantum yield; light-emitting diode; flexible; waterproof;

Abstract

The development of flexible displays for wearable electronics applications has created demand for high-performance quantum dot (QD) light-emitting diodes (QLEDs) based on QD core@shell structures. Emerging indium phosphide (InP)-based core@shell QDs show promise as lighting material in the field of optoelectronics because they are environmentally friendly material, can be produced in a cost-effective manner, and are capable of tunable emission. While efforts have been made to enhance the performance of InP-based QLED, the stabilities of InP@ZnSeS QDs film and InP@ZnSeS-based QLED in water/air are not yet fully understood, limiting their practical applications. Herein, a highly durable, flexible InP@ZnSeS QLED encapsulated in an ultrathin film of CYTOP, a solution-based amorphous fluoropolymer, is demonstrated. The CYTOP-encapsulated green flexible QLED shows an external quantum efficiency (EQE) of 0.904% and a high luminescence of 1593 cd/m^2 as well as outstanding waterproof performance. The flexible device emits strong luminescence after being immersed in water for ~20 minutes. Even when subjected to continuous tensile stress with a 5 mm bending radius, the high luminescence is preserved. This waterproof architecture can be a promising strategy for wearable electronics applications.

Flexible and wearable electronics is underpinning the development of future healthcare and communication technologies based on seamless and non-invasive remote sensing platforms.[1,2] Recent progress on flexible displays has been critical in the use of wearable devices to directly monitor the wearer's vital signs, health- and fitness-related data, location, and other information from sensing platforms which can be bodily worn. Quantum dot (QD) light-emitting diodes (QLEDs) exhibit unique optoelectronic properties including color tunability,[3-6] outstanding color purity,[7] high quantum yield ($\geq$ 70%),[8] and photo stability,[9] printability,[10,11] ultra-thin active layers,[12] and high luminescence at low threshold voltage (up to ~200,000 cd/m^2 and $V_{turn\text{-}on}$ < 2 V),[13-15] making them ideal for exploring novel flexible displays. QDs are fluorescent semiconductor nanocrystals with diameters ranging from 2 – 10 nm. QD core materials include cadmium selenide, indium phosphide (InP), zinc sulfide (ZnS), perovskite, copper indium gallium sulfide, and silicon nanoparticles. Further advances on the QD core@shell technology to which novel high-performance QLED is highly sought are projecting this research field to the new frontiers of flexible QLED display for omnipresent wearable electronics.

To date, the highest QLED external quantum efficiencies (EQEs) have been obtained in Cd-based blue, green and red QLEDs (21.4[16], 27.6[16], and 30.9%[17], respectively). Perovskite is an emerging material in the field of fluorescent semiconductor nanocrystal QLED as well as of solar cell, and EQE of perovskite-based QLEDs has exceeded 10%.[18,19] However, the use of heavy metals such as Cd and Pb in omnipresent consumer electronics has been limited by the European Union's Restriction of Hazardous Substances Directive because of their intrinsic toxicity under the circumstances that has been profusely demanded for the commercial application of heavy metal-based QLEDs.[20,21] InP QDs are a promising alternative to heavy metal-based QDs because of their intrinsic low toxicity and tunable emission from the visible to near-infrared region. The EQEs of QLEDs based on InP QDs have increased consistently from $\leq$ 0.01% to 12.2% (maximum EQEs of 12.2% for the red QLED and 6.3% for the green

QLED) based on improvements in QD synthesis techniques and device structural optimization.[21-28]

These improvements in InP QDs hold promise for the development of flexible QLEDs as wearable displays in healthcare applications. The first steps towards flexible InP QLEDs were achieved by Lim et al. at 2013.[23] However, despite the recent progress in flexible InP QLEDs,[23,29-31] the performance of their devices and encapsulation/characterization technique that provides high water/air stability to allow the electronic devices to be exposed to perspiration, dust, and mechanical stress during daily use, are still in infancy. Therefore, it is important to find encapsulation strategies to protect flexible InP-based QLEDs from water for a long time and to develop characterization technique for investigating waterproof behavior of them.

Herein, we demonstrate highly performed flexible green InP@ZnSeS QLEDs and a facile, effective, and reproducible way to protect and characterize them in water for the first time. Green InP@ZnSeS core@shell semiconductor nanocrystals with a photoluminescence quantum yield (PLQY) of 82% were synthesized via hot-injection. Solution-based flexible InP@ZnSeS QLEDs were fabricated via spin-coating. The resulting flexible green-emitting QLEDs exhibited an EQE of 0.904% and a maximum luminance of 1593 cd/m^2. An ultrathin (thickness = 450nm) film of CYTOP, an amorphous fluoropolymer, was used as the encapsulation layer on the top of the QLEDs, allowing the flexible QLED to operate in water for 40 min. This strategy is expected to pave the way for a new generation of flexible InP-based QLEDs for use in wearable and healthcare applications. These devices will benefit from the environmentally friendly and cost-effective route of QD production along with the scalable and reproducible method used to encapsulate the device in the ultrathin CYTOP film.

The InP core and InP@ZnSeS QDs were synthesized via hot-injection, as shown in **Figure 1**a (see details on the method used to synthesize the QDs in the Supporting Information). The ultraviolet–visible (UV-vis) absorption and photoluminescence (PL) spectra of the InP core and

InP@ZnSeS core@shell QDs were observed (Figure 1b,c). In the UV-vis absorption spectra, the first excitonic peak located at 423 nm in the spectrum of the InP core and 480 nm in the spectrum of the InP@ZnSeS core@shell QDs were red-shifted. Similar phenomena were observed in the PL spectra; the PL peaks position of InP core and InP@ZnSeS core@shell QDs were at ~485 nm and ~537 nm, respectively. These results indicate that quantum confinement was reduced by increasing the nanoparticle size.[30] Additionally, coating the InP core with the ZnSeS shell increased the PLQY from 7% to 82%, which was attributed to the increased crystallinity and compensation of surface defects on the InP core upon coating with the ZnSeS shell.[23]

The identification and crystallinity of the QDs were evaluated by X-ray diffraction (XRD) and transmission electron microscopy (TEM). InP core corresponded to (111), (200), (220), and (311) planes of the face-centered cubic (zinc-blende) structure (JCPDS 32-0452),[32,24] and the peaks were broadened as a result of the low crystalinity (Figure 1d). In InP@ZnSeS core@shell, peaks of the InP core and ZnSe (JCPDS 37-1463) and ZnS (JCPDS 05-0566) shell were observed, corresponding to the (111), (220), and (311) faces. These ZnSe and ZnS peaks are attributed to coating the ZnSe/ZnS gradient shell[32,24]. Since the crystal structures of InP and ZnX (X = S and Se) are essentially same, ZnSeS was selected as a shell layer to reduce the lattice mismatch with InP core; however, their lattice constants were different,[32,24] meaning that the peak positions of InP and ZnSeS do not overlap (Figure 1d). TEM images of both QDs are shown in Figure 1e,f. The InP core and InP@ZnSeS QDs exhibited circular shapes with size of 3 and 4–5 nm, respectively. The low crystallinity of InP core observed by TEM agrees well with the peak broadening observed in the XRD spectrum of the InP core (the fast Fourier transform (FFT) of inset and image in Figure 1e). In contrast, nanocrystal InP@ZnSeS QDs with high crystallinity were observed, as shown in the high resolution and the FFT image (insets of Figure 1f), in agreement with the XRD spectrum of the core@shell QDs. Therefore, coating the InP core with the ZnSeS shell dramatically changed the properties of the QD core as a

photoemissive layer for QLEDs as follows (Figure 1b–e): 1) Compensating for surface defects on the InP core[33]; 2) suppressing lattice mismatch between the core and shell based on gradient shell growth[34]; and 3) improving the optical propertie by type I structure of core@shell, which is both the conduction and valence band edges of ZnSeS shell lie over the bandgap of the core (the inset of Figure 1c), due to fewer interactions of core-localized e-h pairs (excitons) with surface traps than with bare QDs.[33]

CYTOP is a soluble fluoropolymer with excellent water and oil repellency along with chemical and thermal resistance, mechanical strength, and electrical properties as a gate insulator. Thus, CYTOP was selected as a flexible encapsulation layer to fabricate the waterproof, flexible QLEDs. CYTOP exhibits outstanding behavior as a flexible encapsulation layer compared to various polymers reported in the literature, including poly(methyl methacrylate), polyvinyl acetate, poly(dimethoxysilane), and SU-8.[35,36] We investigated CYTOP layers with thicknesses of hundreds of nanometers because polymer layers with thicknesses exceeding 780 nm could be decoupled from the stiff glass substrate, exposing the device to water or oxygen.[37] **Figure 2**a–c show atomic force microscopy (AFM) images of the CYTOP films resulting from deposition by spin coating at 2k, 3k, and 4k rpm to charaterize the surface morphology and thickness. The film thicknesses were obtained from the line profiles to be ~450 nm at 2k, ~340 nm at 3k, and ~300 nm at 4k (Figure 2d,e). The highest CYTOP roughness was observed at 4k as result of particles and holes on the surface (see the insets in Figure 2a–c and e). We also characterized the optical properties of CYTOP films spin-coated onto quartz and Corning glass substates, as shown in Figure 2f. The transmittances of the CYTOP films at 2k, 3k, and 4k rpm were 89.7%, 91.2%, and 91.3% @ 550 nm, respectively. Interestingly, the transmittance of the bare quartz substrate (88.9%) was slightly lower than that CYTOP coated quartz, in agreement with a previous study.[38] Additionally, we observed no absorbance peaks of core@shell QDs film in the green line spectrum of inset in Figure 2f, compared to the blue line spectrum (CYTOP/QD film). QDs film uncoated with CYTOP on the

Corning glass was exposed to air for the tranmittance measurement, and we found that absorbance peaks of QDs film without CYTOP were disappeared, indicating unstability of InP@ZnSeS QDs in air. We applied the CYTOP film with a thickness of 450 nm and a roughness of 0.33 nm for the encapsulation of InP@ZnSeS and its QLED.

Before evaluating the waterproof behavior of the CYTOP-coated QLED, we investigated the stability of InP@ZnSeS QDs with and without CYTOP coating by immersing the QDs in water. The degradation of normalized PL intensity and PLQY, which is defined as the number of photons emitted as a fraction of the number of photons absorbed, was observed as function of immersion time in water (Figure 2g,h). The PL peaks of the QDs coated and uncoated with CYTOP were both observed at 551.3 nm and did not change over 40 min of water immersion, indicating that the water exposure degrades InP@ZnSeS QD via oxidation[39,40] rather than by changing the phase or particle size of the core and shell. The normalized PL intensity of the QDs without CYTOP decreased suddenly with increasing immersion time from 0.4 at 7 min to 0.1 at 40 min. In contrast, the CYTOP-coated InP@ZnSeS QDs exhibited outstanding water repellency due to the surface hydrophobicity of the −CONH~Si(OR)n functional group of M-type CYTOP, as shown in the inset of Figure 2h.[41] The CYTOP-coated QDs maintained a normalized PL intensity over 0.8, even after 40 min of immersion. The initial PLQYs of the uncoated and CYTOP-coated InP@ZnSeS QDs (90.2% and 87.2%, respectively; Figure 2h) were reduced to 12.3% and 78% after 20 min of immersion, respectively. After 40 min, no further PL was observed for the InP@ZnSeS QDs without CYTOP; that is the PLQY was under 10%, corresponding to a 92.5% of reduction. For the CYTOP-coated QDs, the reduction in PLQY after 40 min was only 19.23% (PLQY = 70.3%). The initially lower PLQY of the CYTOP-coated InP@ZnSeS QDs compared to the uncoated QDs was attributed to the spinning process, the exposure to the CYTOP solvent, and light absorption by the CYTOP film. Figure 2i shows the photographs of the pristine quartz and InP@ZnSeS with and without CYTOP. The fluorescence images after 40 min of exposure to water agreed well with the PL and PLQY

results. Therefore, the 450 nm ultrathin CYTOP film was considered to be suitable for the encapsulation of the flexible QLEDs.

A three-dimensional schematic diagram of the regular device structure of the solution-based InP@ZnSeS QLED is shown in **Figure 3**a. QLEDs with the structure (indium thin oxide (ITO)/poly(3,4-ethylenedioxythiophene) polystyrene sulfonate (PEDOT:PSS)/poly(9,9-dioctylfluorene-co-N-(4-butyl-phenyl)diphenylamine) (TFB)/QD/zinc oxide (ZnO)/aluminum (Al)) were fabricated on both glass and polyethylene terephthalate (PET) substrates, and the performance of the device on the glass substrate was evaluated during water immersion for 40 min. To improve the charge recombination efficiency, the QLED contained hole injection layer of PEDOT:PSS, hole transport layer of TFB, and electron transport layer of ZnO layers with the anode (ITO) and cathode (Al) electrode. The lowest unoccupied molecular orbital maximum of TFB (electron affinity = ~2.3 eV) and the valence band minimum of ZnO nanoparticles (ionization potential = ~7.49 eV) fulfill the functions of blocking injected electrons and holes, respectively. The EQEs of the QLEDs showed good reproducibility with an average EQE of 0.67% and a relative standard deviation of 20% (Figure 3b). The maximum EQE was ~1%. Figure 3c–d show the optical behavior and performance of the QLED with an EQE of 0.86%. The luminance consistently increased with increasing operating voltage, reaching 6000 cd/m^2 at 7 V, corresponding to a current density of 295.7 mA/cm^{-2} (Figure 3c). Figure 3d depicts the current efficiency and EQE as functions of the luminance of the device. A current efficiency of 3.36 cd/A and a peak EQE of 0.86% were obtained. The EQE (within ± 5% of variation) was maintained well in the luminance range of 7×10^1 to 8×10^2 cd/m^2. In all fabricated devices, efficiency roll-off at high luminance of QLED was observed. This can be attributed to unbalanced charged injection at high J, which charges QDs and induces Auger recombination,[42,43] and joule heating, which leads to the debonding of ligands, thus

introducing surface traps and consequently decreasing the QY of QDs,[44] in the device, as shown in Figure 3d.

The waterproof behaviors of CYTOP-coated InP@ZnSeS QLEDs on glass and PET substrates for flexible electronics were further investigated. Figure 3e shows current efficiency and EQE as functions of QLED current density for the CYTOP-coated device on a glass substrate after different immersion times in water. The encapsulated QLED exhibited peak EQEs of 0.63%, 0.47%, and 0.38% and current densities of 2.3, 1.73, and 1.39 cd/A after 0, 12, and 40 min of immersion time, respectively. The peak EQE and current efficiency of the device submerged in water for 40 min were approximately 39.7 % and 39.6 % lower than those of the reference device (before soaking in water), respectively. This indicates that the CYTOP-coated QLED still worked after being exposed to water for 40 min. We investigated the waterproof behaviors of several QLEDs with and without CYTOP by measuring their EQEs after various water immersion times (Figure 3f). After 40 min of immersion, an average of EQEs of CYTOP-coated QLEDs was 43% lower than before immersion, and the devices still emitted light. In contrast, the EQEs of the devices without CYTOP encapsulation were reduced by 80% after 1 min of water immersion compared to before immersion, and some devices emitted no light eventually.

Finally, we investigated the performance and waterproof behavior of the solution-based InP@ZnSeS flexible QLED fabricated on a PET substrate and encapsulated with CYTOP. **Figure 4**a shows a photograph of lightening CYTOP-encapsulated flexible QLEDs with a bending radius of 5 mm. The EQEs of the flexible QLEDs showed good reproducibility with an average EQE of 0.49% and a relative standard deviation of 15% (Figure 4b). Figure 4c shows the EL spectra of QLEDs fabricated on PET and glass and PL spectrum of green QDs in solution. The peak wavelength and FWHM of EL data of flexible QLEDs are ~545 nm and ~45 nm, respectively (see the details in table 1 of the Supporting information). The EL spectra showed red-shift (8 nm) and slightly broadening compared with the PL spectra of QDs (peak wavelength: ~537 nm and FWHM: ~43 nm) in solution, which is attributed to the interdot interactions in close packed solid films, dielectric dispersion and the electric-filed-induced

Stark effect.[45] In addition to, we obtained current density-voltage-luminance characteristic of highly performed flexible QLEDs (a high peak EQE of 0.904% and maximum luminance of 1593 cd/m^2) and summarized the key performance parameters of these devices in Figure S1 and table 2 and 3 of Supporting information. We had a lifetime test of flexible QLEDs with CYTOP encapsulation film in air, based on the time-decay model which was previously proposed by Féry et al.[46] (see Figure S2 in the Supporting information) before immersion in water. At fixed 6.7 mA/cm^2, an initial luminance was decreased to 0.95 (L/L_0) over 1 hour (Figure 4d), which means that it allowed flexible QLEDs to be tested on waterproof behavior in water without itself degradation, starting at that current density. As the initial luminance increased by 300 cd/m^2, the half lifetime (LT0.5) was suddenly decreased. The bent green QLED was exposed to water and operated for 40 min at a fixed voltage (current density stared at 6.7 mA/cm^2) (see the video in the Supporting Information). Images from the captured video are shown in Figure 4e. After 40 min of immersion in water, the luminance of the flexible QLED with a bending radius of 5 mm decreased significantly, and nearly half of the luminescent area did not emit light. This might be attributed to penetration of water molecules in the active layer interfaces induced by the mechanically stressed device. Figure 4f shows the J/J_0 ratio as functions of the time in water and air of the flexible QLED. Generally, to verify CYTOP as the encapsulation layer, the lifetime at which the EL intensity (or luminance) of the QLED decreases to 50% of the initial value should be measured.[12,14] We found that ~40% reduction of current density of the flexible QLEDs corresponded to half of a luminance after 12 to 20 min of water immersion. Therefore, we inferred the lifetime of the flexible QLED to be ~17 min (estimated LT0.5 at 0.6 J/J_0). The degradation mechanism can be described as follows. Water molecules penetrate through the defect points such as nano-scale cracks or pin holes in the 450 nm CYTOP film, leading to the degradation of QLED.[47-49]

In summary, we demonstrated a facile, effective, and reproducible way to deposit an ultrathin film of CYTOP as an encapsulation layer to protect flexible green InP@ZnSeS QLEDs

from water. Green InP@ZnSeS core@shell QDs as an environmentally friendly material were synthesized via hot-injection method and exhibited a PLQY of 82%. The CYTOP-coated QDs exhibited outstanding water stability, as indicated by PLQY characterization. After immersion in water for 40 min, the PLQY of the QDs was reduced by only 19.23 %. The highly performed flexible green InP@ZnSeS QLEDs fabricated by all-solution processes had maximum EQEs of 0.904% and luminance of 1593 cd/m^2. The flexible CYTOP-encapsulated green InP@ZnSeS QLED with a bending radius of 5 mm was submerged in water and operated constantly for 40 min. This work constitutes a new step toward the realization of waterproof QLED displays that could be integrated with a wide range of wearable and flexible devices.

Acknowledgements

D-W. S. and Y-H. S. contributed equally to this work. The authors acknowledge the support from European Commission Horizon2020 under grant agreement number (685758). The research leading to these results received funding from Engineering and Physical Sciences Research Council (EPSRC) project reference of EP/P027628/1 for funding the 'Smart Flexible Quantum Dot Lighting' used in this research.

References

[1] D.-W Shin, M. D. Barnes, K. Walsh, D. Dimov, P. Tian, A. I. S. Neves, C. D. Wright, S. M. Yu, J.-B. Yoo, S. Russo, M. F. Craciun, *Adv Mater.* **2018**, *20*, 1802953.

[2] H. Chen, J. He, R. Lanzafame, I. Stadler, H. E. Hamidi, H. Liu, J. Celli, M. R. Hamblin, Y. Huang, E. Oakley, G. Shafirstein, H.-K Chung, S.-T. Wu, Y. Dong, *J. Soc. Inf. Display* **2017**, 25, 177

[3] S. Coe-Sullivan, *Nat. Photonics* **2009**, *3*, 315.

[4] D. V. Talapin, J.-S. Lee, M. V. Kovalenko, E. V. Shevchenko, *Chem. Rev.* **2010**, *110*, 389.

[5] A. P. Alivisator, *Science* **1996**, *271*, 933.

[6] N. Tessler, V. Medvedev, M. Kazes, S. Kan, U. Banin, *Science* **2002**, *295*, 1506.

[7] Z. Chen, B. Nadal, B. Mahler, H. Aubin, B. Dubertret, *Adv. Func. Mater.* **2014**, *24*, 295.

[8] I. Mekis, D. V. Talapin, A. Kornowski, M. Haase, H. Weller, *J. Phys. Chem. B* **2003**, *107*, 7454.

[9] J. M. Caruge, J. E. Halpert, V. Wood, V. Bulovic,, M. G. Bawendi, *Nat. Photonics* **2008**, *2*, 247.

[10] W. K. Koh, S. R. Saudari, A. T. Fafarman, C. R. Kagan, C. B. Murray, *Nano Lett.* **2011**, *11*, 4764.

[11] D. K. Kim, Y. Lai, B. T. Diroll, C. B. Murray, C. R. Kagan, *Nat. Commun.* **2012**, *3*, 1216.

[12] Q. Sun, Y. A. Wang, L. S. Li, D. Wang, T. Zhu, J. Xu, C. Yang, Y. Li, *Nat. Photonics* **2007**, *1*, 717.

[13] J. Kwak, W. K. Bae, D. Lee, I. Park, J. Lim, M. Park, H. Cho, H. Woo, D. Y. Yoon, K. Char, S. Lee, C. Lee, *Nano Lett.* **2012**, *12*, 2362.

[14] L. Qian, Y. Zheng, J. Xue, P. H. Holloway, *Nat. Photonics* **2011**, *5*, 543.

[15] B. S. Mashford, M. Stevenson, Z. Popovic, C. Hamilton, Z. Zhou, C. Breen J. Steckel, V. Bulovic, M. Bawendi, S. Coe-Sullivan, P. T. Kazlas, *Nat. Photonics* **2013**, *7*, 407.

[16] H. Zhang, S. Chen, X. W. Sun, *ACS nano* **2018**, *12*, 697.

[17] a) J. Song, O. Wang, H. Shen, Q. Lin, Z. Li, L. Wang, X. Zhang, L. S. Li, *Adv. Func. Mater.* **2019**, 29, 1808377; b) K. Ding, Y. Fang, S. Dong, H. Chen, B. Luo, K. Jiang, H. Gu, L. Fan, S. Liu, B. Hu, L. Wang, *Adv. Opt. Mater.* **2018**, *6*, 1800347.

[18] N. Wang, L Cheng, R. Ge, S. Zhang, Y. Miao, W. Zou, C. Yi, Y. Sun, Y. Cao, R. Yang, Y. Wei, Q. Guo, Y. Ke, M. Yu, Y. Jin, Y. Liu, Q. Ding, D. Di, L. Yang, G. Xing, H. Tian, C. Jin, F Gao, R. H. Friend, J. Wang, W. Huang, *Nat. Photonics* **2016**, *10*, 699.

[19] S. Lee, J. H. Park, Y. S. Nam, B. R. Lee, B. Zhao, N. Di, E. D. Jung, H. Jeon, J. Y. Kim, H. Y. Jeong, R. H. Friend, M. H. Song, *ACS nano*, **2018**, *12*, 3417.

[20] W. Shen, H. Tang, X. Yang, Z. Cao, T. Cheng, X. Wang, Z. Tan, J. You, Z. Deng, *J. Mater. Chem. C.* **2017**, *5*, 8243.

[21] H. Zhang, N. Hu, Z. Zeng, Q. Lin, F. Zhang, A. Tang, Y. Jia, L. S. Li, H. Shen, F. Teng, Z. Du, *Adv. Optical Mater.* **2019**, *7*, 1801602.

[22] J. Lim, W. K. Bae, D. Lee, M. K. Nam, J. Jung, C. Lee, K. Char, S. Lee, *Chem Mater.* **2011**, *23*, 4459.

[23] J. Lim, M. Park, W. K. Bae, D. Lee, S. Lee, C. Lee, K. Char, *ACS nano* **2013**, *7*, 9019.

[24] F. Gao, S. Wang, F. Wang, Q. Wu, D. Zhao, X. Yang, *Chem, Mater.* **2018**, *30*, 8002.

[25] K. R. Reid, J. R. McBride, N. J. Freymeyer, L. B. Thal, S. J. Rosenthal, *Nano Lett.* **2018**, *18*, 709.

[26] P. Ramasamy, N. Kim, Y. S. Kang, O. Ramirez, J. S. Lee, *Chem. Mater.* **2017**, *29*, 6893.

[27] M. D. Tessier, E. A. Baquero, D. Dupont, B. Grigel, E. Bladt, S. Bals, Y. Coppel, Z. Hens, C. Nayral, F. Delpech, *Chem. Mater.* **2018**, *30*, 6877.

[28] Y. Li, X. Hou, X. Dai, Z. Yao, L. Lv, Y. Jin, X. Peng, *J. Am. Chem. Soc.* **2019**, *141*, 6448.

[29] Y. Kim, T. Greco, C. Ippen, A. Wedel, M. S. Oh, C. J. Han, J. Kim, *Nanoscience and Nanotechnology Lett.* **2013**, *5*, 1065.

[30] D. Hahm, J. H. Chang, B. G. Jeong, P. Park, J. Kim, S. Lee, J. Choi, W. D. Kim, S. Rhee, J. Lim, D. C. Lee, C. Lee, K. Char, W. K. Bae, *Chem. Mater.* **2019**, *31*, 3476.

[31] J.-W. Kim, J. Kim, *J. Vac. Sci. Tech. B* **2017**, *35*, 04E101.

[32] Y. Kim, S. Ham, H. Jang, J. H. Min, H. Chung, J. Lee, D. Kim, E. Jang, *ACS Appl. Nano Mater.* **2019**, *2*, 1496.

[33] P. Reiss, M. Protiere, L. Li, *Small* **2009**, *5*, 154.

[34] F. Pietra, L. De Trizio, A. W. Hoekstra, N. Renaud, M. Prato, F. C. Grozema, P. J. Baesjou, R. Koole, L. Manna, A. J. Houtepen, *ACS nano* **2016**, *10*, 4754.

[35] J. Granstrom, J. S. Swensen, J. S. Moon, G. Rowell, J. Yuen, A. J. Heeger, *Appl. Phys. Lett.* **2008**, *93*, 193304

[36] L. Wang, C. Ruan, M. Li, J. Zou, H. Tao, J. Peng, M. Xu, *J. Mater. Chem. C* **2017**, *5*, 4017.

[37] A. Bulusu, A. Singh, C. Y. Wang, A. Dindar, C. Fuentes-Hernandez, H. Kim, D. Cullen, B. Kippelen, S. Graham, *J. Appl. Phys.* **2015**, *118*, 085501.

[38] H. Cheema, J. H. Delcamp, *Adv. Energy. Mater.* **2019**, *9*, 1900162.

[39] R. P. Brown, M. J. Gallagher, D. H. Fairbrother, Z. Rosenzweig, *Langmuir* **2018**, *34*, 13924.

[40] A. Tarantini, K. D. Wegner, F. Dussert, G. Sarret, D. Beal, L. Mattera, C. Lincheneau, O. Proux, D. Truffier-Boutry, C. Moriscot, B. Gallet, P.-H. Jouneau, P. Reiss, M. Carriere, *NanoImpact* **2019**, *14*, 100168.

[41] J. B. Chae, J. O. Kwon, J. S. Yang, D. Kim, K. Rhee, S. K. Chung, *Sensors & Actuators: A. Physical* **2014**, *215*, 8

[42] W. K. Bae, Y. S. Park, J. Lim, D. Lee, L. A. Padilha, H. McDaniel, I. Robel, C. Lee, J. M. Pietryga, V. I. Klimov, *Nat. commun.* **2013**, *4*, 2661.

[43] J. Lim, Y.-S. Park, K. Wu, H. J. Yun, V. I. Klimov, *Nano Lett.* **2018**, *18*, 6645.

[44] H. Moon, C. Lee, W. Lee, J. Kim, H. Chae, *Adv. Mater.* **2019**, *31*, 1804294.

[45] P. Ramasamy, K.-J. Ko, J.-W. Kang, J.-S. Lee, *Chem. Mater.* **2018**, *30*, 3643.

[46] C. Féry, B. Racine, D. Vaufrey, H. Doyeux, S. Cinà, *Appl. Phys. Lett.* **2005**, *87*, 213502.

[47] M. Schaer, F. Nüesch, D. Berner, W. Leo, L. Zuppiroli, *Adv. Func. Mater.* **2001**, *11*, 116.

[48] S. Sato, S. Ohisa, Y. Hayashi, R. Sato, D. Yokoyama, T. Kato, M. Suzuki, T. Chiba, Y. Pu, J. Kido, *Adv. Mater.* **2018**, *30*, 1705915.

[49] Y. Wang, J. He, H. Chen, J. Chen, R. Zhu, P. Ma, A. Towers, Y. Lin, A. J. Gesquiere, S.-T. Wu, Y. Dong, *Adv. Mater.* **2016**, 28, 10710.

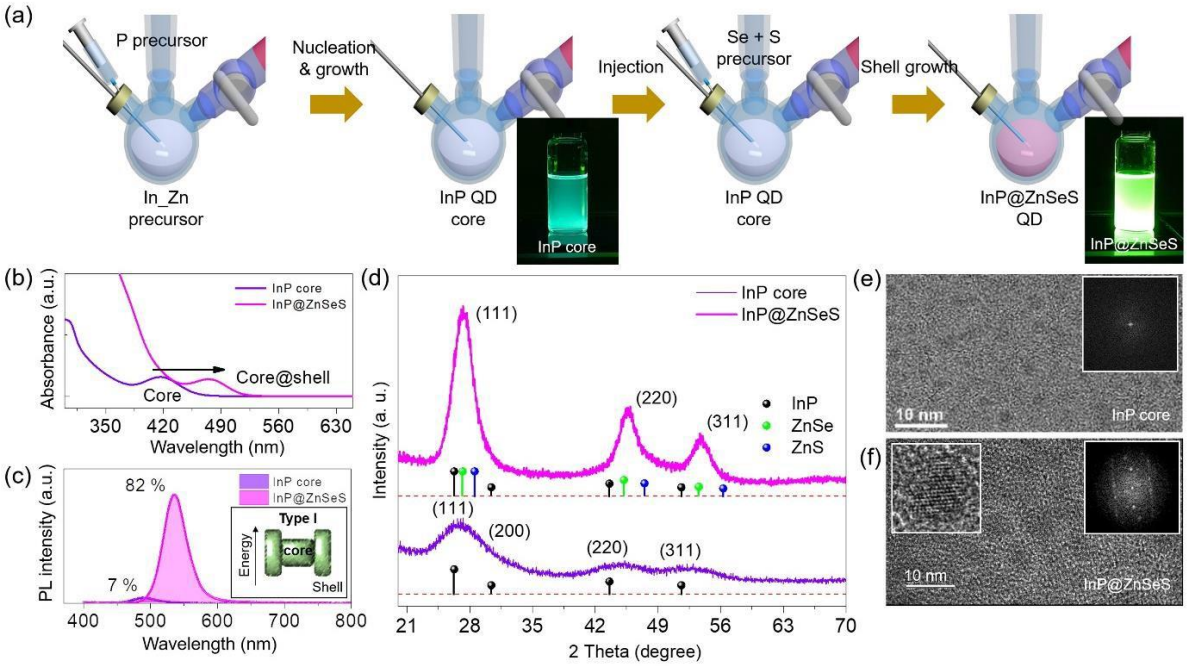

Figure 1. Synthesis and characterization of InP core and InP@ZnSeS core@shell QDs. a) Schematic of the synthetic processes of InP core and InP@ZnSeS core@shell QDs and fluorescence images of both QDs under UV illumination. Optical properties of the InP core and InP@ZnSeS core@shell QDs: b) UV-vis absorbance and c) PL. Identification and crystallinity evaluation of the QDs: d) XRD spectra and TEM images of the e) InP core and f) InP@ZnSeS core@shell QDs. The insets in e) and f) are the diffraction patterns of both QDs along with a high resolution TEM image of the core@shell QDs (top-left inset in f).

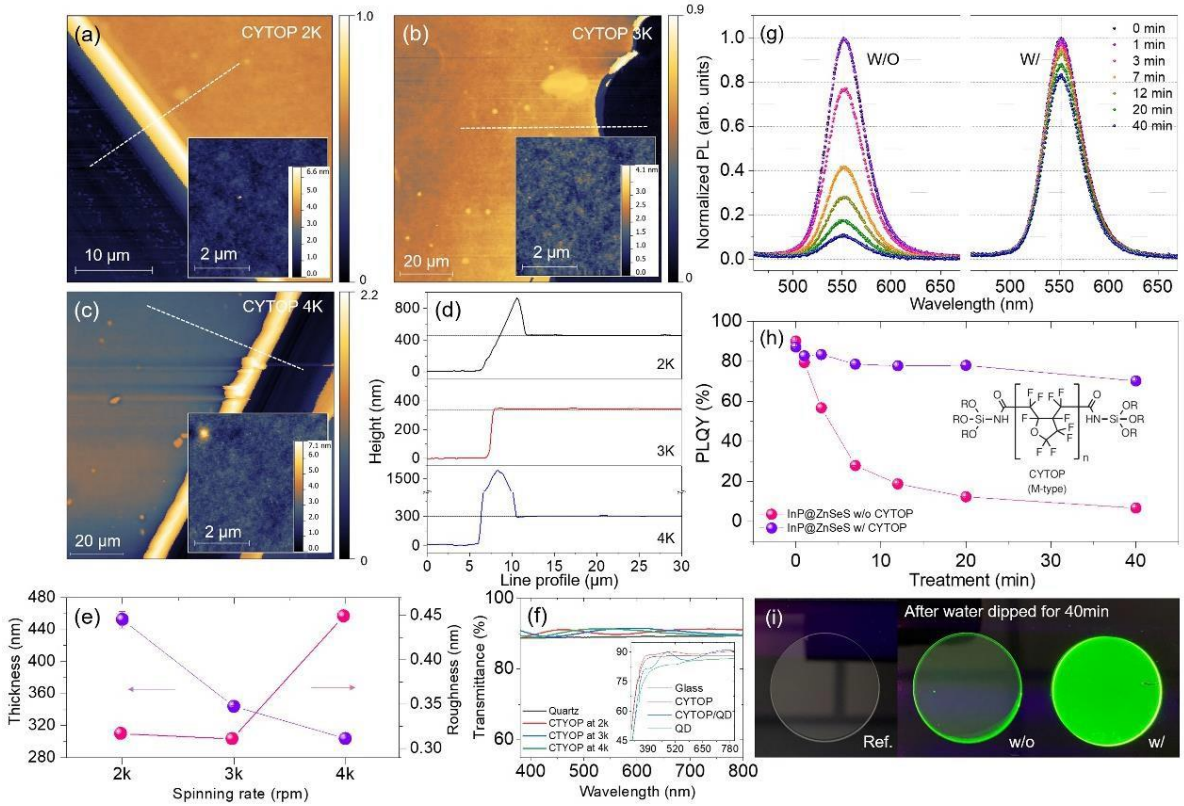

Figure 2. Characterization of CYTOP films spin-coated at various speeds and waterproof CYTOP-encapsulated InP@ZnSeS QDs immersed in water. AFM images of CYTOP coated on quartz substrates at various spin speeds: a) 2000, b) 3000, and c) 4000 rpm. The insets in a–c are AFM images of the CYTOP surface. d) Line profiles, e) thickness and roughness, and f) transmittance of the CYTOP films deposited at various spin speeds. The inset in f) compares the tranmisttance profiles of CYTOP-encapsulated QDs and uncoated QDs. g) Normalized PL spectra and h) PLQY values of InP@ZnSeS on a quartz substrate with and without CYTOP encapsulation during immersion in water for 40 min. i) Fluorescence images of bare quartz and InP@ZnSeS on quartz with and without CYTOP encapsulation under long-wave UV irradiation (365 nm).

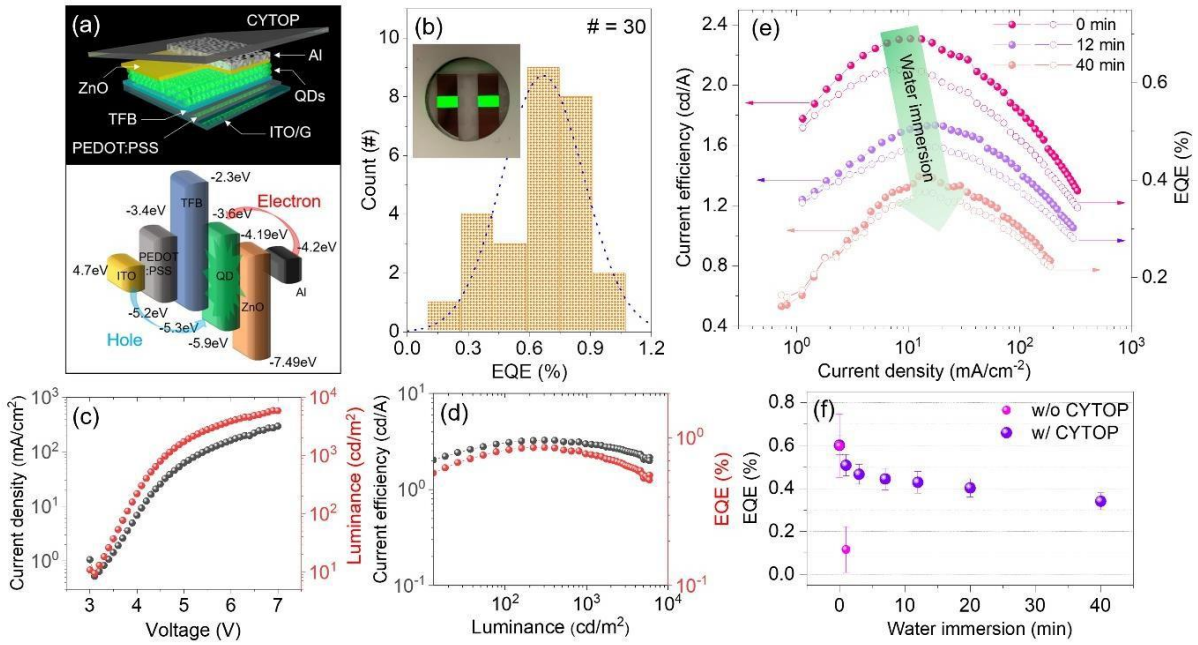

Figure 3. Images and charaterization of a waterproof CYTOP-encapsulated InP@ZnSeS QLED on glass . a) Schematic of the device structure and the corresponding energy band diagram. b) Histogram showing the maximum peak of EQE measured from 30 devices with the same structure. The inset of b) shows a photograph of EL emission from the device operated at 5 V. c) Current density–luminance–voltage characteristics of the device. d) Current efficiency and EQE as functions of device luminance. Performance of an InP@ZnSeS QLED on glass as functions of immersion time in water: e) Current efficiency and EQE of the devices as functions of current density. f) EQE of CYTOP-encapsulated QLED as functions of immersion time in water.

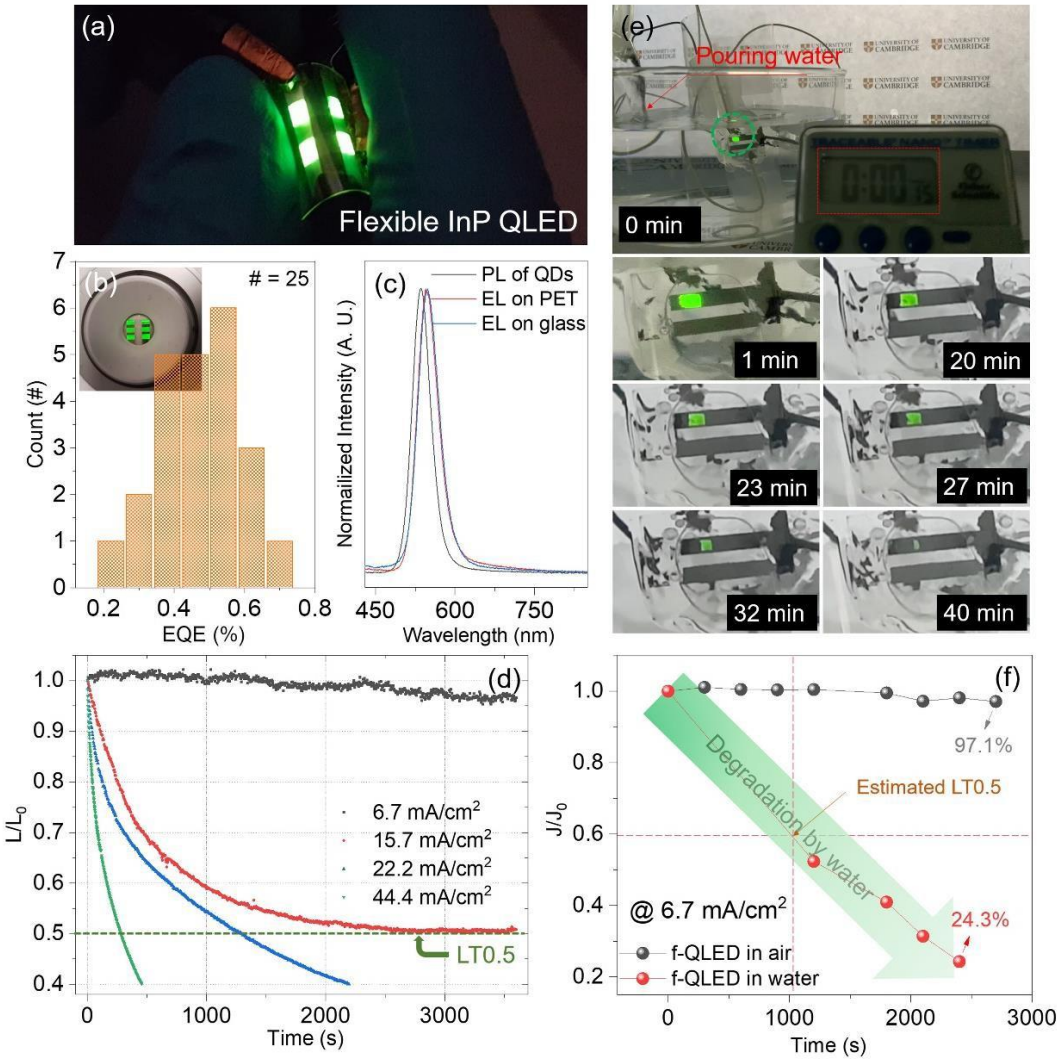

Figure 4. a) A typical photoimage of the waterproof CYTOP encapsulated flexible QLED on the PET with a bending radius of 5 mm. b) Histogram showing the maximum peak of EQE measured from 25 devices with the same structure. The inset of b) shows a photograph of EL emission from the device operated at 7 V. c) PL of QDs solution and EL spectra of QLED on PET and glass. d) Lifetime (LT) test of flexible QLEDs at 6.7, 15.7, 22.2, and 44.4 mA/cm^2. e) Photographs of the CYTOP-encapsulated flexible device in water during different immersion times in water from 0 min to 40 min. f) Flexible QLEDs were tested in air and water at fixed voltage (starting at 6.7 mA/cm^2). J/J_0 ratio of the encapsulated flexible device as functions of operation time in air and water.